

COVER PAGE

Document downloaded by @DAEL

Sun Nov 29 12:28:37 2026
For personal use

When automatic English translation is provided, only the original document is authentic.
The EAA cannot be held responsible of any translation error

Bibliographical reference

Spectral Enrichment of Transient Acoustic Waves as a Function of Input Signal Shape, Pablo L. Rendón, Carlos G. Malanche, Felipe Orduña-Bustamante and Antonio Pérez-López, Acta Acustica **vol. 103** (Number 3), 2017, pp. 379-384

DOI
https://doi.org/10.3813/AAA.919067

Acta Acustica united with Acustica
Vol. 103 (2017) 379 – 384

DOI 10.3813/AAA.919067

Spectral Enrichment of Transient Acoustic Waves as a Function of Input Signal Shape

Pablo L. Rendón, Carlos G. Malanche, Felipe Orduña-Bustamante, Antonio Pérez-López
Grupo de Acústica y Vibraciones, Centro de Ciencias Aplicadas y Desarrollo Tecnológico, Universidad Nacional Autónoma de México, Ciudad Universitaria, A.P. 70-186, México D.F. 04510, México. pablo.rendon@ccadet.unam.mx

Summary
Nonlinear acoustic propagation effects are known to account for waveform steepening for sufficiently intense signals having travelled over a long enough distance. This steepening, which will eventually produce a shock wave, results, in turn, in a transfer of energy to the high end of the frequency spectrum. The shock formation distance, however, is inversely proportional not to the maximum amplitude of the waveform, but to its maximum slope. We test this theoretical result by producing two sets of short pulses in a long cylindrical tube, where the energy content of each pulse in a set is constant, but the maximum slope varies. The pulses are allowed to propagate over a distance long enough for nonlinear steepening to become apparent. We observe the expected result, where for an initially loud signal the value of the maximum slope does affect the rate at which energy is pumped to high frequencies, whereas for a signal with much smaller initial energy content it does not. This result is of interest in the context of musical acoustics, as it confirms recent observations where players of some brass instruments can affect the brightness of their sound purely through slight changes in embouchure [16].

PACS no. 43.25.-x, 43.25.Zx, 43.58.Ry, 43.75.-z, 43.75.Fg

1. Introduction

It is generally acknowledged that nonlinear propagation effects must be taken into account for the description of sufficiently intense acoustic waves travelling over long distances. This is typically the case for aeroacoustic noise generated by aircraft turbines, but, at a much smaller scale, nonlinear effects are also observed in the context of sound propagating in long, narrow tubes. Finite-amplitude sound waves propagating in waveguides with slowly-varying nonrectangular cross sections have been studied widely, amongst others by Chester [6, 7] and Keller [12], and they are mainly characterised by nonlinear steepening of the wave profiles over distance. This steepening can eventually lead to the formation of a shock wave, but even before a shock is formed, it results in a significant transfer of energy towards the higher-end of the frequency spectrum associated with the time signal. Spectral enrichment, in turn, provides a second criterion, besides waveform steepening, for the detection of nonlinear propagation effects, but it is also probably the most noticeable consequence of these effects from the standpoint of a listener.

A well-known example of a cylindrical waveguide where the effects of nonlinear steepening become apparent is the slide trombone, where it has been shown by Hirschberg et al [11] that shocks form inside the resonator at *fortissimo* level. The spectral enrichment at high frequencies which accompanies nonlinear propagation is responsible for the particular quality of sound of trombones and other brass instruments achieved when they are played loudly, and which is known as ”brassy” sound [10]. Not all of the causes of the distinctly bright sound of brass instruments when played loudly are due to nonlinear propagation effects, however. The nonlinearity of the source itself has been established for both trumpets and trombones [1, 9], and Poirson et al [17] have shown that the geometry of the mouthpiece may also contribute to the perceived brightness of the sound. In addition, a couple of factors determine the extent to which nonlinearity affects the propagation of acoustic waves, apart from sheer intensity. Myers et al [15] have shown that analysing the shape of the wind instruments under consideration is extremely important in order to assess the scale of the nonlinear effects associated with propagation inside the instrument. Nonlinear propagation effects are most clearly present in instruments with a long cylindrical section, such as the trombone and the trumpet [18]. In brass instruments, it is also possible to control the degree of brightness through embouchure control, modifying both tension in the lip muscles and the angle of the mouthpiece [5]. By doing so, players are changing not so much the amplitude, but rather the gradient of the input pressure signal in such a manner that a bright sound can be produced even at *mezzo forte* playing levels [16].

Received 7 October 2016,
accepted 11 March 2017.

© S. Hirzel Verlag · EAA

This behaviour is easily explained by examining the expression for the shock formation distance in a pipe with uniform cross section where no losses occur [11]. This last assumption, regarding the lack of either viscothermal losses is justified and discussed in detail by Msallam et al [14]. The shock formation distance, x_s, is then obtained through the method of characteristics, by explicitly calculating the initial distance at which the wave profile becomes multivalued as a result of progressive steepening, and it is given, in terms of the input pressure, p_{in}, by:

$$x_s \approx \frac{2\,\gamma\,c_0\,p_0}{(\gamma+1)\left(\partial p_{in}/\partial t\right)_{\max}}, \qquad (1)$$

where t is time, γ is the Poisson constant for air, c_0 is the local sound speed, and p_0 is the atmospheric pressure [21]. This distance can serve as a useful indicator of the scale of nonlinear steepening to which a transient wave is subjected, as a small value of x_s generally indicates a greater degree of nonlinear steepening taking place than a larger value of x_s. The wave steepens as it travels, but clearly, at any given point, the degree of steepening it has undergone also depends on how steep it was to begin with. Thus, although a large amplitude of the input pressure is clearly necessary in order to observe nonlinear propagation effects, it is actually the maximum value of the temporal gradient of the input pressure which determines the scale of these effects (see the denominator on the right-hand side of equation (1) above).

In this paper, we test the hypothesis that the shape of the input pressure signal is the dominant factor when establishing the scale of nonlinear steepening, rather than solely the amplitude of the signal. To this end, we consider a low-intensity regime, where the root mean square (rms) pressure of the input signals is moderate, and a high-intensity regime, where the rms pressure of the signals is high. In each case, we produce a series of short pulses with approximately the same energy content, but with different maximum values of the temporal gradient of the input pressure, and record these input pulses at an initial location very close to the source. We then let these pulses propagate along a length of cylindrical tubing considered long enough to allow for the effects of nonlinear steepening, if at all present, to become apparent, and compare the pulses recorded at this fixed distance with the input pulses. Since the pulse that has travelled a longer distance has been subjected to the effects of viscothermal attenuation, the values of the maximum slope after the pulse has travelled a certain distance will be smaller than the initial values of the maximum slope, but in the high-intensity regime we still expect steepening to counteract the effect of attenuation to some noticeable degree. Perhaps a better measure of the scale of nonlinear distortion which affects the travelling pulses in this regime will be obtained by analysing the spectrum of these time signals, as nonlinear steepening of the wave profile is typically accompanied by a transfer of energy to high frequencies [8]. The low-intensity regime is used as a control sequence, where we expect little-to-no nonlinear steepening to occur, but for the high-intensity sequence we do expect to observe an increase in the scale of nonlinear steepening, and the accompanying spectral enrichment, with increasing maximum temporal gradient of the input signal.

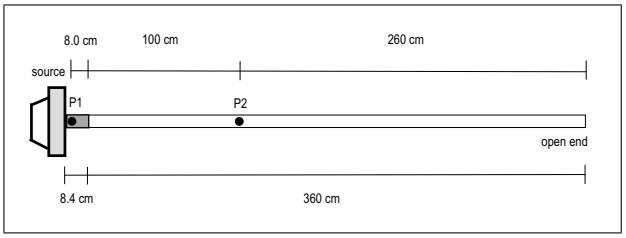

Figure 1. Diagram illustrating measurement positions along the length of the cylindrical pipe.

2. Experimental set-up

We used a very similar set-up to that used previously by Rendón et al [18, 19] to produce short pulses inside a 3.6 m-long cylindrical tube with an internal diameter of 13.9 mm and an open end. Since we are interested in establishing the extent to which nonlinear effects alter the profiles of waves propagating along a cylindrical duct, we must be able to isolate progressive waves travelling towards the open end of the tube. Rather than use a two-microphone method to separate ingoing and outgoing waves [20], we simply ensure that the pulses are short enough to be treated as transients which do not interfere with one another after reflection from the open end of the tube. Sound excitation is provided by a Radson U150 S driver, coupled to the tube by means of an 8.4 cm PVC cylindrical tube with an internal diameter of 10.7 mm made especially for this purpose. Sound pressure measurements were obtained with a Brüel & Kjaer type 4182 probe microphone at two different positions along the cylindrical pipe, where, in both cases, the probe microphone was inserted and plasticine was used to seal the space around the probe, thus approximating continuous closed bore conditions. For the first position, closest to the driver and labelled from here on as position 1, a 1.5 mm diameter hole was drilled on to the cylindrical fitting part 4 mm from the driver exit. A second hole, corresponding to position 2, was drilled at a distance of 1.0 m from the beginning of the cylindrical pipe. The distance between position 2 and the open end of the tube is thus sufficiently large to guarantee that, provided that the pulses are not longer than 10 ms, there will be no overlap due to the reflected pulse at position 2. A diagram of the set-up, including the measurement positions, is shown in Figure 1.

Input signals, which are typically less than five milliseconds long, were generated using a Stanford research DS345 function generator and a Yamaha AX-380 power amplifier. The measurements were then acquired by means of a Brüel & Kjaer type 2034 dual-channel analyser, and transferred to a laptop computer through a National Instruments GPIB/IEEE-488.1 interface.

3. Experimental procedure and results

3.1. Generation of short pulses

Sequences of short rectangular pulses of varying voltages and durations were produced in the function generator for both the low-intensity (linear) and the high-intensity (nonlinear) regime, manually adjusting the duration and amplitude levels of the pulses so that their rms energy content, measured at position 1, was constant for each regime, even while tweaking their shape. The duration of these pulses at position 1 was always less than 10 ms so that an interval of this fixed length, $t_2 - t_1 = 10$ ms, could then be used in all cases to calculate the rms value of the pressure, given by:

$$p_{rms}(t) = \left[\frac{1}{t_2 - t_1}\int_{t_1}^{t_2} p(t)^2\,\mathrm{d}t\right]^{1/2}. \qquad (2)$$

Observe that it is sufficient, for the purpose of comparing rms pressures, to compute only the value of the integral in (2). After the rms pressure of the initial pulse in the sequence was calculated, the next pulse was generated with a slightly longer duration. The voltage was then adjusted in such a manner that the rms pressure equalled, to within 1% error, the value obtained during the initial measurement. This adjustment was generally achieved through trial and error by decreasing the voltage from its previous level in small steps until the desired value was obtained. As the pulses enter the pipe, they have already been subjected to a large amount of distortion, due mostly to the dynamics of the driver itself, the geometry of the driver casing, and the coupling with the pipe. Further, the low voltages associated with the linear regime give rise to a highly irregular response of the speaker coil, and it becomes difficult to produce different rectangular pulses with identical values of the rms pressure. Thus, the larger amplitude of the high-amplitude pulses affords greater freedom when modifying the shape of the pulses, so that it was possible to produce 12 distinct pulses with different values of the maximum temporal gradient, whereas for the low-intensity sequence it was only possible to produce 5 distinct pulses. The rms pressure of the low-intensity pulses was 4.8 Pa (108 dB) and that of the high-intensity pulses was 2585.4 Pa (162 dB), with an error of less than 1% in both cases. Each measurement initially consists of the average of 100 pulse-synchronised sound pressure transients, with a further ten measurements made and averaged for each hole, taking out and reinserting the probe on each occasion, so that this new average takes into account the statistical effect of small changes in microphone position. The shape of the pulses as they enter the pipe, measured at position 1, can be seen in Figure 2.

3.2. Results

The expected steepening of high-intensity pulses as they propagate along the tube is readily apparent in Figure 2, while in the same figure it can be seen that low-intensity pulses do not exhibit the same behaviour. In order to make

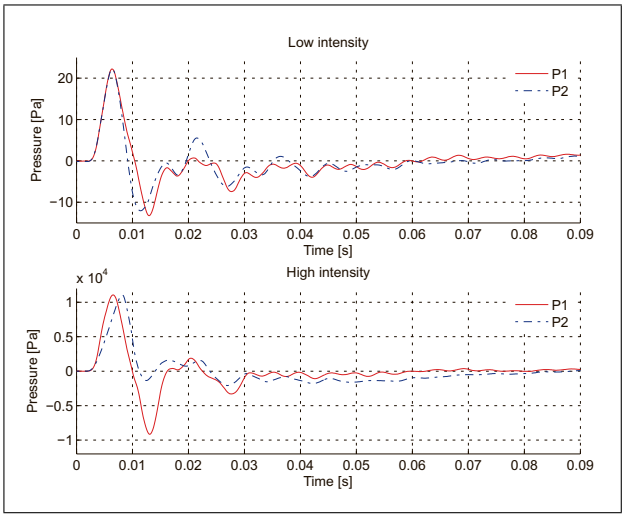

Figure 2. (Colour online) Time signals for the low-intensity and high-intensity pulses at positions 1 and 2, aligned at the start of the rise of the first peak. The time signals at position 2 are scaled to have the same maximum value as the signals at position 1.

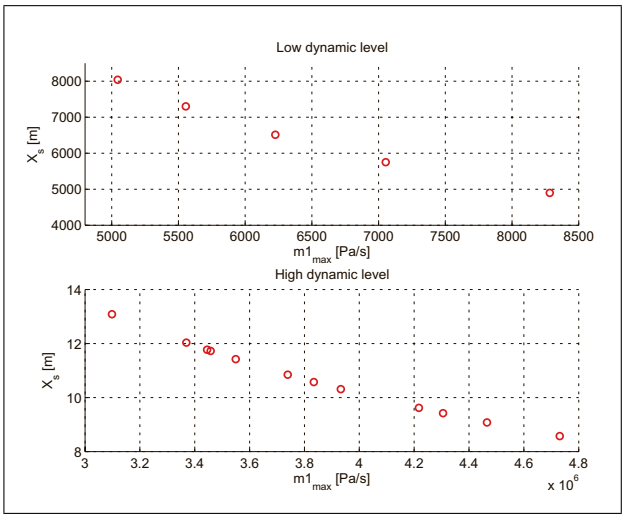

Figure 3. (Colour online) Shock formation distance x_s as a function of the maximum gradients of time-signals at position 1, for both the low- and the high-intensity regimes.

the comparison as objective as possible, each of the initial pulses portrayed in this figure is the steepest member of its respective sequence. The effect of attenuation is considerable for these pulses even at this relatively short distance, so we have scaled the pulses observed at position 2 so as to have the same maximum amplitude as the pulse observed at position 1. A measure of the scale of the nonlinear steepening expected for both the low-intensity and the high-intensity pulses is illustrated in Figure 3, where the shock formation distance x_s, defined above in (1), is plotted against the maximum temporal gradient of signals at position 1, $m1_{max}$. We observe that for the linear case a shock will effectively never develop, while for the nonlinear case a shock will form after a distance of only a few meters, so we do expect nonlinear steepening to be already noticeable at position 1. It is not immediately evi-

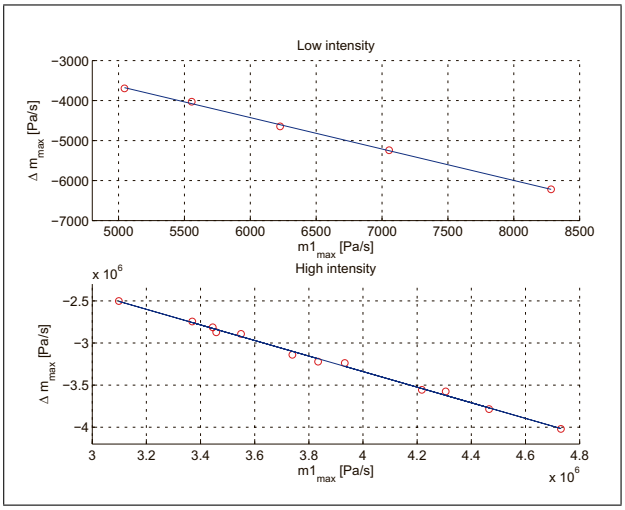

Figure 4. (Colour online) Difference between the maximum gradients of time-signals at positions 2 and 1, as a function of maximum gradient at position 1, for both the low- and the high-intensity regimes.

dent from either of these plots, however, that in the nonlinear regime steeper initial pulses should be associated with a faster steepening of the wave profile and, as a consequence, greater rates of transfer of energy to the high-end of the frequency spectrum.

In order to examine the rate at which energy is pumped to high frequencies in the nonlinear regime, consider the quantity $\Delta m_{max} = m2_{max} - m1_{max}$, the difference between the maximum slopes at positions 2 and 1, $m2_{max}$ and $m1_{max}$ respectively. Because of viscothermal attenuation, the travelling pulses will have a much smaller maximum temporal gradient at position 2 than at position 1. According to a simple model of attenuation in ducts [13, 22, 4], if x_1 and x_2 are the distances corresponding to positions 1 and 2, then the attenuation which affects the pulses between positions 1 and 2 is given by a factor of the form $\exp[-\alpha_1 \sqrt{f}\,(x_2 - x_1)]$, where f is the frequency and α_1 is a positive constant which depends on both the physical properties of the medium and the geometry of the tube. If we denote the Fourier transform of the pressure as $\tilde{p}$, we can write

$$\tilde{p}(x_2, f) = \mathrm{e}^{-\alpha_1 \sqrt{f}\,(x_2 - x_1)}\, \tilde{p}(x_1, f). \tag{3}$$

The values of $m1_{max}$ and $m2_{max}$ can then be calculated as

$$\begin{aligned} m1, 2_{max} &= \left| \frac{\partial p(x_{1,2}, t)}{\partial t} \right|_{max} = \left[2\pi f\, \mathcal{P}_{1,2}(f) \right]_{max} \\ &= 2\pi f_{1,2}\, \mathcal{P}_{1,2}(f_{1,2}), \end{aligned} \tag{4}$$

where $\mathcal{P}_{1,2}$ represent the magnitude of the Fourier transforms of p at positions 1 and 2, respectively. In order to calculate Δm_{max} we use equations (3) and (4) to obtain

$$\Delta m_{max} = 2\pi f_2\, e^{-\alpha_1 \sqrt{f_2}\,(x_2 - x_1)}\, \mathcal{P}_1(f_2) - m1_{max}. \tag{5}$$

In the linear regime, because the distance between positions 1 and 2 is not large, we may assume that $f_2 = f_1 + \Delta f$, where Δf is very small. Substituting this expression for f_2 in equation (5), we obtain

$$\begin{aligned} \Delta m_{max} = {} & 2\pi f_1\, \mathcal{P}_1(f_1) \left[1 - \alpha_1 \sqrt{f_1}\,(x_2 - x_1) \right] \\ & - m1_{max} + O(\Delta f). \end{aligned} \tag{6}$$

We now use (4) once more to arrive at

$$\Delta m_{max} = -\alpha_1 \sqrt{f_1}\,(x_2 - x_1)\, m1_{max} + O(\Delta f). \tag{7}$$

Thus, we expect Δm_{max} to decrease linearly with increasing $m1_{max}$. This behaviour is indeed observed in Figure 4, where linear regression gives coefficients of determination $R^2 = 0.99$ for both linear and nonlinear regimes. The dimensionless slopes of these straight lines are, in the linear case -0.7849, and in the nonlinear case -0.9246. That the gradient corresponding to high intensities is larger in absolute value than that corresponding to low intensities is consistent with the assumption that nonlinear steepening is taking place in the first case, but not in the second. Note that in both cases, the largest values of $m1_{max}$ are over 50% larger than the smallest values of the same variable, so for both regimes we cover approximately the same range of values of this quantity as do Norman et al [16] in their paper.

In order to gauge the rate at which energy is transferred to the high-end of the frequency spectrum as the maximum initial slope of the aforementioned pulses increases, we have calculated the spectral centroid (SC) of each of these time signals, which is a measure of the brightness, or spectral enrichment, of the signal [2]. Spectral centroids were calculated from the average sound pressure pulses by multiplying by a Tukey time window, which is flat in the first half, corresponding to the high amplitude parts of the measured pulses, and attenuates as a half-wave raised cosine (like a Hanning window) in the second half, where measured pulses also decay. Frequency analysis of the discrete Fourier quadratic spectrum was restricted to the range below 2000 Hz for the calculation of the spectral centroids, which appear below 1000 Hz in all cases.

The following expression was used:

$$f_c = \sum_{f_k = 100\ \mathrm{Hz}}^{2000\ \mathrm{Hz}} f_k \left| P(f_k) \right|^2 \Bigg/ \sum_{f_k = 100\ \mathrm{Hz}}^{2000\ \mathrm{Hz}} \left| P(f_k) \right|^2, \tag{8}$$

where $P(f_k)$ are the frequency components of the discrete Fourier spectrum of the average sound pressure signal $p_{\mathrm{av}}(t_n)$, with a sampling frequency $f_s = 65,536$ Hz, and a frequency resolution close to $\Delta f_k = 100$ Hz. The frequency limits, 100–2000 Hz, were chosen so as to include most of the higher amplitude components of $|P(f_k)|^2$, while avoiding those with lower amplitudes, at lower and higher frequencies, where background noise could affect the calculation. Wider frequency limits were found to have little effect in the resulting spectral centroids.

A signal with large gradients will typically have a larger spectral centroid than a flatter signal, with less pronounced gradients. Since the amplitude of the low-intensity pulses

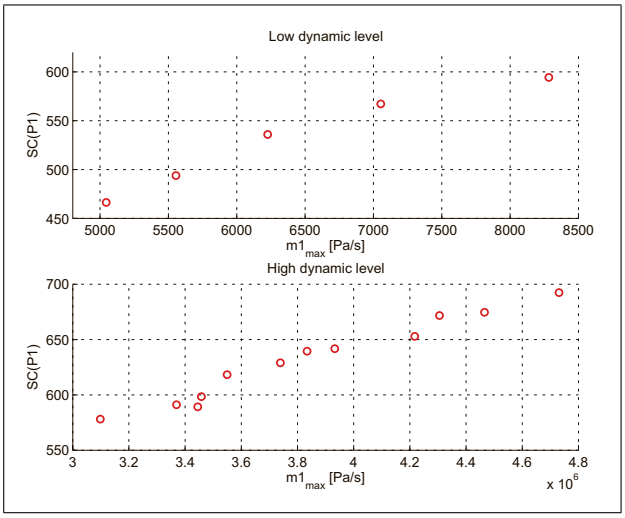

Figure 5. (Colour online) Spectral centroid as a function of maximum gradient at position 1, for both the low- and the high-intensity regimes.

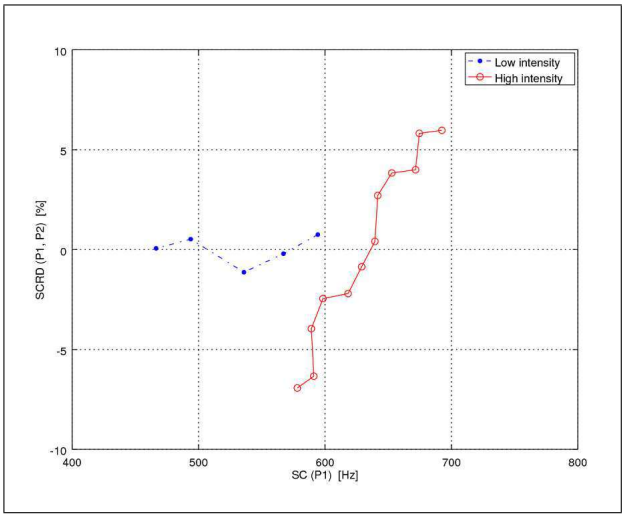

Figure 6. (Colour online) Spectral centroid ratio drift between positions 1 and 2 as a function of initial spectral centroid for both the low-intensity and the high-intensity regime.

is smaller than that of the high-intensity pulses, the spectral centroids associated with the former generally have smaller values than those associated with the latter. Thus, as the maximum slope of the pulses measured at P1 increases, so does the spectral centroid associated with these pulses. We have checked that higher values of $m1_{max}$ do indeed correspond to larger spectral centroids, as we would expect them to, and we have plotted the results, for both regimes, in Figure 5.

Calculating the spectral centroids for transient signals can be problematic for low-amplitude signals, as Beauchamp [2] has pointed out, if background noise attains a sound pressure level comparable in order to that of the time signal itself. High-frequency noise, mechanical vibrations from the experimental set-up, or even an irregular response from the driver may produce low-amplitude peaks in the spectrum which will nonetheless shift the spectral centroids up or down, depending on the position of the peaks. For the purposes of this paper, we are interested not in the values of the spectral centroids as such, but rather in establishing whether varying the maximum temporal gradient of a signal affects the displacement of the spectral centroids at a fixed propagation distance. For this reason, we calculate the ratio of spectral centroids between positions 1 and 2 relative to the mean value of the whole sequence, for both the low- and high-amplitude cases. We call this quantity, which is expressed in percentage points below and above the mean, the spectral centroid ratio drift (SCRD), and plot its values for both sequences, as functions of initial maximum temporal slope, in Figure 6.

In the linear regime we observe that the points related to this sequence lie along a horizontal straight line, representing zero drift, so that increasing the maximum temporal gradient of these signals does not result in an increase in the rate of transfer of energy to the high-end of their spectra. The tendency of the points associated with the nonlinear regime, on the other hand, is clearly increasing, so we may then conclude that increasing the maximum temporal gradient of a signal does affect the rate at which energy is pumped to the high-end of its frequency spectrum. As we have mentioned above, the effect of viscothermal damping increases with frequency, and signals with larger maximum temporal gradients at position 1 have greater energy content in the higher frequencies. Thus, as $m1_{max}$ increases, viscothermal losses contrive to diminish the energy content of the high end of the frequency spectrum more rapidly. Nonlinear steepening must then be responsible for the observed transfer of energy to the higher frequencies and, as we hypothesised earlier, this transfer occurs more quickly for signals which are already steeper initially.

4. Conclusion

We have examined how varying the shape of a pulse affects the scale of nonlinear steepening to which it is subjected as it travels along a fixed length of cylindrical tubing, producing both low- and high-intensity pulses in order to be able to isolate the effects of nonlinear propagation. In the time domain, we have compared in straightforward manner the maximum temporal gradients of the pulses at both observation positions, obtaining the expected result, namely, that increasing maximum initial slopes leads to quicker profile distortion in the nonlinear case than it does in the linear case. This result, however, does not prove that the accelerated rate at which energy is transferred to high frequencies for larger inital slopes is due to nonlinear steepening. To prove this, we must look at the frequency domain, where we have established that the maximum temporal gradient of the initial signals only plays a part in the manner in which energy is transferred to the higher frequencies in the nonlinear regime, again, as expected. For this purpose we introduced a dimensionless quantity, the spectral centroid ratio drift, which is a measure of the spec-

tral enrichment of a single signal relative to a given group of signals, at a fixed propagation distance. We then examined, for both sequences of measurements, the relationship between this parameter and the initial spectral centroid, which is, in a sense, simply the centre of mass of the frequency spectrum of the initial signal. The increasing relationship between these two quantities observed in the nonlinear regime confirms our hypothesis that it is the initial shape of a signal, rather than solely its energy content, which determines the scale of nonlinear propagation effects. These results are very much in line with those reported by Norman et al [16], where it is established that the shape of the signal produced at the entrance to the instrument has an influence on the scale of the nonlinear propagation effects observed in the instruments at *mezzo forte* and *fortissimo* levels.

Acknowledgement

The authors acknowledge the financial support provided by DGAPA-UNAM through project PAPIIT IN109214.

References

[1] J. Backus, T. C. Hundley: Harmonic generation in the trumpet. J. Acoust. Soc. Am. **49** (1971) 509–519.

[2] J. W. Beauchamp: Synthesis by spectral amplitude and "brightness" matching of analyzed musical instrument tones. J. Audio Eng. Soc. **30** (1982) 396–406.

[3] A. H. Benade: On woodwind instrument bores. J. Acoust. Soc. Am. **31** (1959) 137–146.

[4] A. H. Benade, D. J. Gans: Sound production in wind instruments. Ann. N. Y. Acad. Sci. **155** (1968) 247–263.

[5] D. M. Campbell, C. A. Greated: The Musician's Guide to Acoustics. Oxford University Press, New York, 1987.

[6] W. Chester: Resonant oscillations in closed tubes. J. Fluid Mech. **18** (1964) 44–66.

[7] W. Chester: Nonlinear resonant oscillations of a gas in a tube of varying cross-section. Proc. Roy. Soc. A **444** (1994) 591–604.

[8] D. G. Crighton: Nonlinear acoustics, in Modern Methods in Analytical Acoustics. Springer-Verlag, New York, 1992.

[9] S. Elliott, J. Bowsher, P. Watkinson: Input and transfer response of brass wind instruments. J. Acoust. Soc. Am. **72** (1982) 1747–1760.

[10] J. Gilbert, L. Menguy, D. M. Campbell: A simulation tool for brassiness studies. J. Acoust. Soc. Am. **123** (2008) 1854–1857.

[11] A. Hirschberg, J. Gilbert, R. Msallam, A. P. J. Wijnands: Shock waves in trombones. J. Acoust. Soc Am. **99** (1996) 1754–1758.

[12] J. B. Keller, M. H. Milman: Finite-amplitude sound-wave propagation in a waveguide. J. Acoust. Soc. Am. **49** (1971) 329–333.

[13] G. Kirchhoff: Über den Einfluss der Wärmeleitung in einem Gase auf die Schallbewegung. Annalen der Physik und Chemie **134** (1868) 177–193.

[14] R. Msallam, S. Dequidt, R. Caussé, S. Tassart: Physical model of the trombone including nonlinear effects. Application to the sound synthesis of loud tones. Acta Acust. united with Acust. **86** (2000) 725–736.

[15] A. Myers, R. W. Pyle, J. Gilbert, D. M. Campbell, J. P. Chick, S. Logie: Effects of nonlinear sound propagation on the characteristic timbres of brass instruments. J. Acoust. Soc. Am. **131** (2012) 678–688.

[16] L. Norman, J. P. Chick, D. M. Campbell, A. Myers, J. Gilbert: Player control of 'brassiness' at intermediate dynamic levels in brass instruments. Acta Acust. united with Acust. **96** (2010) 614–621.

[17] E. Poirson, J. F. Petiot, J. Gilbert: Study of the brightness of trumpet tones. J. Acoust. Soc. Am. **118** (2005) 2656–2666.

[18] P. L. Rendón, R. Ezeta, A. Pérez-López: Nonlinear sound propagation in trumpets. Acta Acust. united with Acust. **99** (2013) 607–614.

[19] P. L. Rendón, F. Orduña Bustamante, D. Narezo, A. Pérez-López, J. Sorrentini: Nonlinear progressive waves in a slide trombone resonator. J. Acoust. Soc. Am. **127** (2010) 1096–1103.

[20] A. F. Seybert, D. F. Ross: Experimental determination of acoustic properties using a two-microphone random-excitation technique. J. Acoust. Soc. Am. **61** (197) 1362–13707

[21] G. B. Whitham: Linear and Nonlinear Waves. Wiley Interscience, New York, 1974.

[22] C. Zwikker, C. W. Kosten: Sound Absorbing Materials. Elsevier, New York, 1949.